2.3   IMPACTS OF THE DECEMBER 2006 SOLAR RADIO BURSTS ON GPS OPERATIONS

Charles S. Carrano[*] and Christopher T. Bridgwood
Atmospheric and Environmental Research, Inc., Lexington, MA

Keith M. Groves
Air Force Research Laboratory, Space Vehicles Directorate, Hanscom AFB

1. ABSTRACT

Four very intense X class solar flares originated from active sunspot region 10930 on December 5, 6, 13, and 14 of 2006. The solar radio bursts associated with the solar flares on December 6, 13, and 14 radiated enough microwave power and with the proper polarization to cause severe fading of the GPS carrier signals. During these events, each lasting up to an hour, nearly identical patterns of intermittent signal fading were observed along all GPS satellite links from receivers located on the sunlit side of Earth (even from receivers separated by thousands of miles). The depth of these GPS signal fades were modulated by the local solar incidence angle (due to the anisotropy of the GPS antenna gain). The solar radio burst on December 6 was particularly intense and caused GPS signal fades in excess of 25 dB, intermittent loss of lock on several GPS satellites, and outage periods with complete loss of GPS positioning information lasting for several minutes. Peak GPS positioning errors in the horizontal and vertical directions during the event reached approximately 20 and 60 meters, respectively. While deep signal fading of the GPS carrier signals were observed during the solar radio bursts on December 6, 13 and 14, only the December 6 solar radio burst was strong enough to substantially impact GPS tracking and positioning accuracy.

2. INTRODUCTION

In December of 2006, four X class solar flares originated from active sunspot region 10930 on the sun. The solar radio bursts associated with the solar flares on December 6, 13, and 14 were characterized by exceptionally large solar flux levels in the microwave region of the electromagnetic spectrum. Figure 1 shows the GOES solar X-ray flux measured during these four events. While it had been predicted in the late 1990s [Klobuchar et al., 1999] that solar radio bursts could affect GPS performance if the solar flux is sufficiently large in the L band frequency range and with Right Hand Circular Polarization (RHCP) (the polarization to which GPS antennas are

Corresponding author address: Charles S. Carrano, Atmospheric and Environmental Research, Inc., Lexington, MA 02421; e-mail: ccarrano@aer.com.

receptive), the direct effects of a solar radio burst on the reception of the GPS signals was not observed until recently [Cerutti et al., 2006]. In this case, a reduction in the signal to noise ratio of the GPS signals was observed by receivers on the sunlit side of Earth during the solar radio burst on September 7, 2005. This occurred because the solar radio signal acts as elevated background noise which competes with the broadcast GPS signals. Even still, the modest reductions in the signal to noise ratios that were observed on this day had little impact on overall GPS availability or positioning accuracy. The solar radio burst that occurred on December 6 of 2006 was of a very different nature—not only was the reception of GPS signals affected, but it was impacted enough to degrade GPS availability and positioning accuracy for extended periods of time.

The frequency response of a solar radio burst is associated with the altitude within the solar atmosphere where the explosive release of energy takes place [Warmuth and Mann, 2005]. This relationship is due to the variation of the plasma frequency with altitude, which increases with the electron density as the altitude decreases. Solar radio bursts releasing large levels of microwave radiation are typically associated with events that occur near the transition region between the solar corona and chromosphere. Shortly after the solar flares on December 6 and 13 the Optical Solar Patrol Network (OSPAN) optical telescope observed Moreton waves in the Hα, which is sensitive to activity in the chromosphere. This is consistent with the production of large solar flux levels in the microwave region of the spectrum. The authors are not aware of any reported observations of Moreton waves associated with the December 5 and 14 solar radio bursts.

3. INSTRUMENTATION

The AFRL Scintillation Network and Decision Aid (AFRL-SCINDA) is a network of ground-based receivers that monitor trans-ionospheric signals at the VHF and L Band frequencies. It was established by the Air Force Research Laboratory to provide regional specification and short-term forecasts of scintillation caused by electron density irregularities in the equatorial ionosphere [Groves et al., 1997]. The AFRL-SCINDA network currently includes 16 dual-frequency GPS receivers that record the scintillation

Strength	X9.0	X6.5		X3.4	X1.5
Date	Dec 5	Dec 6		Dec 13	Dec 14
Start	10:18	18:29		02:14	21:07
Peak	10:35	18:47		02:40	22:15
Stop	10:45	19:00		02:52	22:26
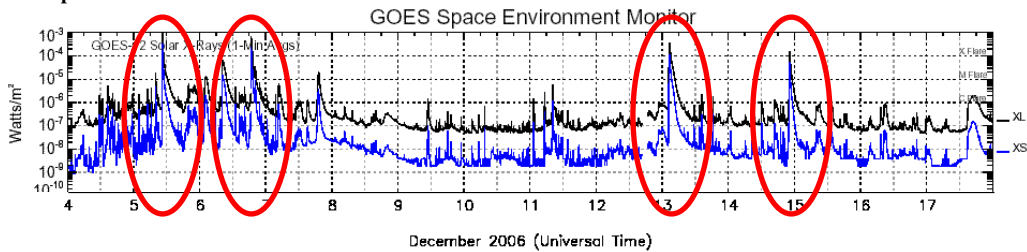
Figure 1. GOES solar X-ray flux showing the strength, start time, time of peak flux, and end time of the four X class solar flares that occurred in December 2006. Figure credit: NOAA's National Geophysical Data Center.

intensity index, S_4, Total Electron Content (TEC), and its rate of change, ROTI, using the full temporal resolution of the receiver hardware (between 10-50 Hz depending on the receiver model). The details of how these parameters are calculated from the raw amplitude, pseudorange, and phase measurements may be found in Carrano [2008] and Carrano et al. [2006]. A map showing the locations of the AFRL-SCINDA ground stations as of April 2007 is shown in Figure 2. Most of the AFRL-SCINDA ground stations are positioned between the ionization crests of the Appleton anomaly, as these locations experience the strongest global levels of ionospheric scintillation.
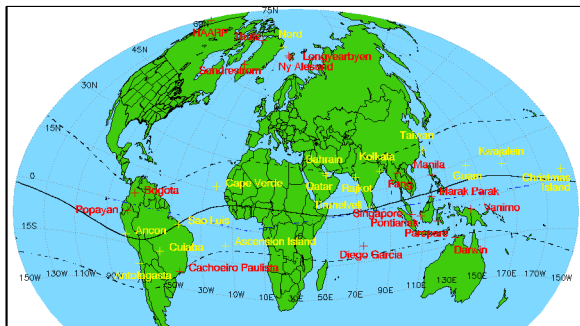
Figure 2. Locations of the AFRL-SCINDA ground stations, as of April 2007. Yellow labels indicate stations equipped with a dual-frequency GPS receiver. The solid and dashed curves show the approximate locations of the geomagnetic equator and the crests of the Appleton anomaly, respectively.

4. DISCUSSION

December 5

The X9.0 solar flare that occurred on December 5, 2006 was the strongest of the four December flares,

at least in terms of X-ray power. It was accompanied by a solar radio burst as well, but the solar radio power in the GPS L1/L2 frequency bands with RHCP was not large enough to cause a detectable fade in the L1 or L2 signals. The SCINDA GPS receiver at Ascension Island was collecting raw 50 Hz measurements during this event. Figure 3 indicates that the L1 and L2 signals were unaffected by the solar radio noise during this event. The solar incidence (zenith) angle at the midpoint of the time period shown (10:45 UT) was approximately 33°.

While the signal to noise ratios of the GPS signals were unaffected by the solar radio burst, the associated solar flare event was, in fact, detectable with a dual frequency GPS receiver because of the enhanced ionization caused by solar EUV radiation. Figure 4 shows the differential pseudorange (in meters) and differential carrier phase (in TEC units) measured during the event. The impulsive enhancement in ionization due to the flare can be seen in the form of a Sudden Increase in TEC (SITEC) starting at about 10:28 UT (which is after the start of the X-ray emission at 10:18 UT and before the peak X-ray emission at 10:35 UT). During this event the TEC increased by approximately 5 TECU in 11 minutes. Note that while both the differential pseudorange and differential carrier phase provide measures of the TEC, the former is not well suited to the detection of small changes in TEC as it is generally noisier due to its increased sensitivity to multipath. Also note that the differential carrier phase provides a measure of relative (uncalibrated) slant TEC only: the geometrical effects due to differing slant path lengths through the ionosphere have not been taken into account, nor have hardware biases associated with the receiver and satellites.

2

L1 ΔC/No

L2 ΔC/No
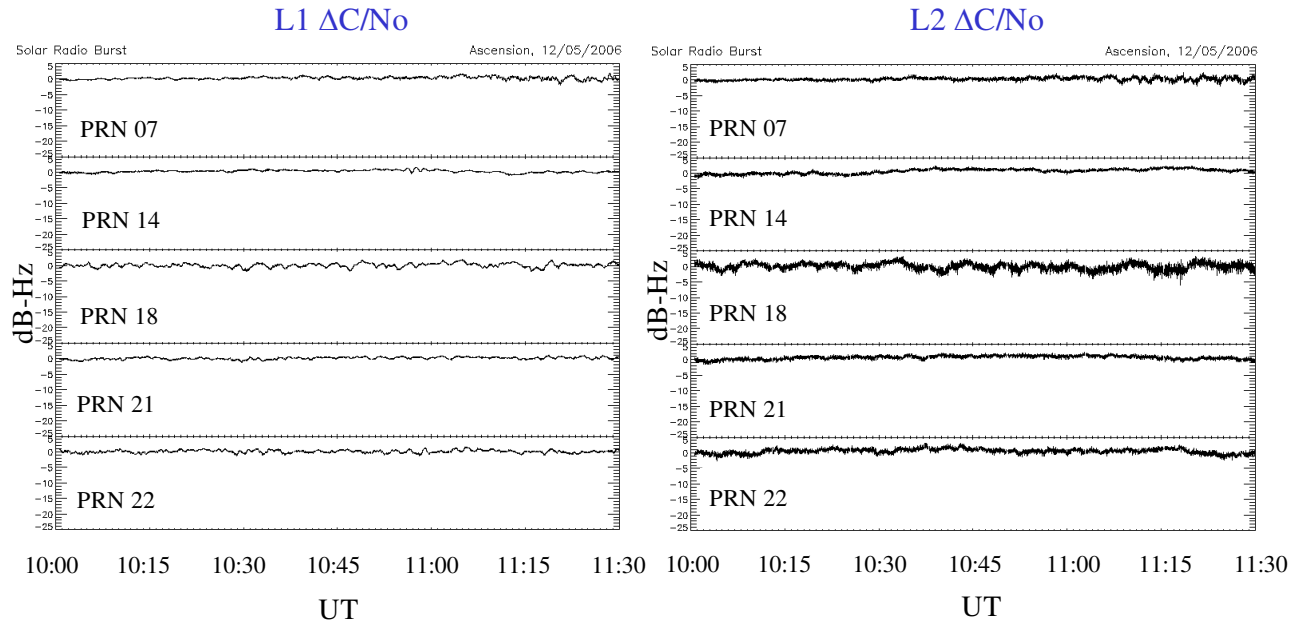
Figure 3. GPS signal fades on the L1 (left) and L2 (right) carriers for a number of GPS satellites (identified by their PRN codes) observed on December 5, 2006 at Ascension Island with a NovAtel GSV 4004B GPS receiver. The solar incidence (zenith) angle at 10:45 UT was approximately 33°.

Differential Pseudorange

Differential Carrier Phase
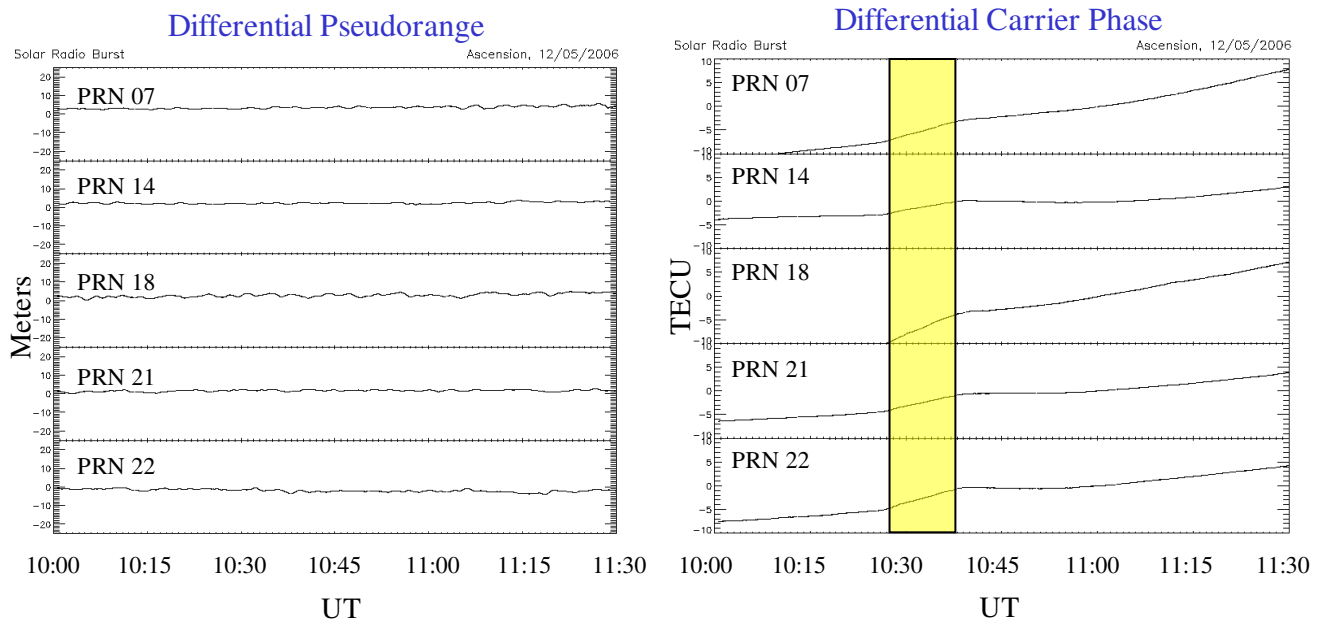
Figure 4. Differential pseudorange (left) and differential carrier phase (right) measured on December 5, 2006 at Ascension Island with a NovAtel GSV 4004B GPS receiver. The yellow shaded region indicates the SITEC event due to enhanced EUV radiation from the solar flare.

3

<u>December 6</u>

The X6.5 solar flare that occurred on December 6, 2005 was associated with a solar radio burst that had the largest impact on GPS signal reception, tracking, and positioning accuracy ever recorded. During the event, the Owens Valley Solar Array measured unusually high levels of RHCP power over a wide range of frequencies in the gigahertz range (Figure 5). This solar radio burst was so intense that difficulties were encountered in calibrating the instrument, and estimations of the absolute RHCP power level were actually obtained using GPS receivers themselves [*Kintner*, 2007]. The peak RHCP power was estimated to exceed 1 million Solar Flux Units (SFU) at the L1 frequency during this event.
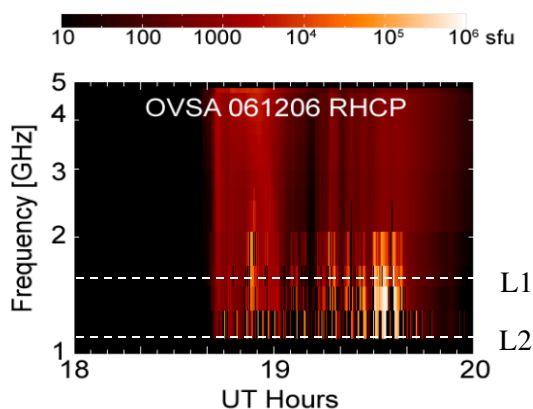
Figure 5. Solar radio burst RHCP power at Gigahertz frequencies on December 6, 2006 measured by the Owens Valley Solar Array operated by NJIT. The dashed lines indicate the GPS L1 (1.575 GHz) and L2 (1.228 GHz) frequencies. The peak power level exceeded 1 million SFU at the L1 frequency. Figure courtesy of D. Gary and P. Kintner.
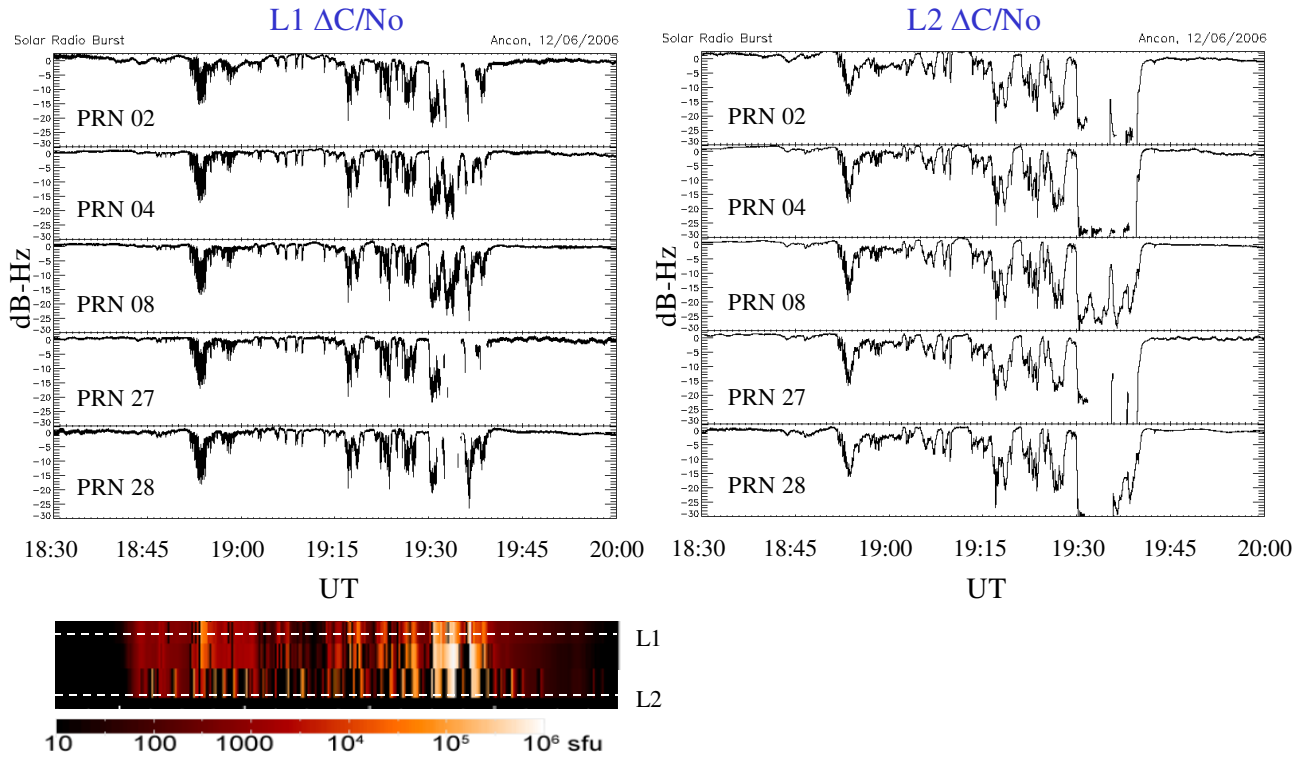
Observations from Ancon, Peru

Figure 6 shows the L1 and L2 signal fades caused by this solar radio burst as observed from Ancon, Peru on December 6, 2006. The solar incidence angle at the midpoint of the time period shown (19:15 UT) was 34°. The GPS receiver model at this station was an Ashtech Z-XII recording data at 20 Hz. A sustained pattern of deep signal fades occurred on both the L1 and L2 channels during this event, lasting for about an hour. As described in *Cerruti et al.* [2006], the fading of GPS signals during an intense burst of solar radio noise occurs due to the response of the Automatic Gain Control (AGC) circuit in the presence of wideband background noise; as the AGC reduces the total power (signal plus background noise) entering at the antenna, the signal to noise ratio of the
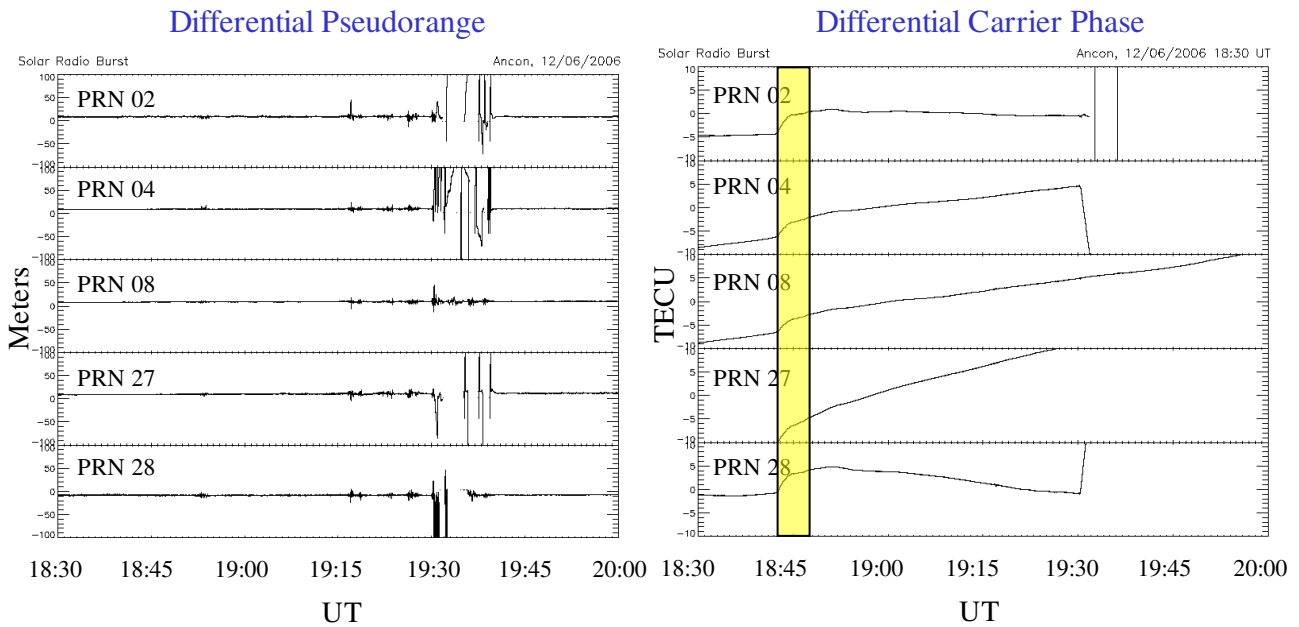
received GPS signal drops. The deepest signal fades on L1 and L2 during this event were measured to be approximately 25 and 30 dB, respectively, while the longest duration fades on L1 and L2 lasted approximately 4 minutes and 9 minutes, respectively. During the periods of strongest solar radio burst power, intermittent loss of lock on the L1 and L2 signals from several GPS satellites occurred, reducing the number of satellites available for computing the receiver position.

Note that the pattern of L1 signal fades is essentially identical for all the GPS satellites for which a lock on the signal is maintained, regardless of their azimuth or elevation. This indicates a source of radio noise entering at the GPS antenna mixing with the signals from each of the satellites, as opposed to, for example, ionospheric scintillation due to electron density irregularities along the path of propagation (which would be different for each satellite link). The signal fades match peaks in the solar radio noise as measured by the OVSA telescope and occur on much longer time scales (up to several minutes) compared with the signal fades typical of ionospheric scintillation which are typically shorter than a second. As we shall see, the depth of signal fading depends on both the solar radio burst RHCP power and the local solar incidence angle. These same arguments apply to the L2 signal fades as well, but since this GPS receiver was not keyed to decode the military (encrypted) Y code, the L2 signal has been measured with less fidelity than the L1 signal (this may be responsible for the somewhat smoother appearance of the L2 fades in comparison with the L1 fades).

The reduction in L1 and L2 signal to noise ratios during the solar radio burst had an adverse effect on the measurement of the GPS observables, namely the pseudoranges and carrier phases. Figure 7 shows the differential pseudorange (in meters) and differential carrier phase (in TEC units) measured during the event for a number of GPS satellites. When the signal fades are deepest (refer to Figure 6), excursions in the measured differential pseudorange occurred, exceeding 100 meters in some cases. These excursions do not accurately reflect the true ionospheric delay (as 100 meters of differential pseudorange would correspond to more than 600 TECU, which is not physical); instead they represent errors in the receiver's measurement of the L1 and/or L2 pseudoranges caused by the low GPS signal strengths. While a GPS receiver typically has internal logic to exclude some false ranging measurements from the calculation of receiver position, some of these ranging errors do contribute, along with the reduction in number of satellites available because of intermittent loss of lock, to increased GPS positioning errors [*Carrano et al.*, 2005].

4

L1 ΔC/No

Ancon, 12/06/2006

PRN 02

PRN 04

PRN 08

PRN 27

PRN 28

dB-Hz

18:30   18:45   19:00   19:15   19:30   19:45   20:00

UT

L2 ΔC/No

Solar Radio Burst   Ancon, 12/06/2006

PRN 02

PRN 04

PRN 08

PRN 27

PRN 28

dB-Hz

18:30   18:45   19:00   19:15   19:30   19:45   20:00

UT

L1

L2

10   100   1000 10^4 10^5 10^6 sfu

Figure 6. GPS signal fades on L1 (left) and L2 (right) for a number of GPS satellites observed on December 6, 2006 at Ancon with an Ashtech Z-XII GPS receiver. The solar incidence (zenith) angle at 19:15 UT was approximately 34°. The color plot at the lower left shows the measured solar radio flux from OVSA between 18:30 and 20:00 UT (the timescale is the same as the other two plots). The plot of OVSA solar radio flux is courtesy of D. Gary and P. Kintner.

Differential Pseudorange

Solar Radio Burst   Ancon, 12/06/2006

PRN 02

PRN 04

PRN 08

PRN 27

PRN 28

Meters

18:30   18:45   19:00   19:15   19:30   19:45   20:00

UT

Differential Carrier Phase

Solar Radio Burst   Ancon, 12/06/2006 18:30 UT

PRN 02

PRN 04

PRN 08

PRN 27

PRN 28

TECU

18:30   18:45   19:00   19:15   19:30   19:45   20:00

UT

Figure 7. Differential pseudorange (left) and differential carrier phase (right) measured on December 6, 2006 at Ancon with an Ashtech Z-XII GPS receiver. The yellow shaded region indicates the SITEC event due to enhanced EUV radiation from the solar flare.

5

The right panel of Figure 7 shows the SITEC event starting at about 18:42 UT (after the start of X-ray emission at 18:29 UT and before the X-ray peak at 18:47 UT) due to enhanced ionization caused by the solar flare's emission in the EUV. During this event the TEC increased by approximately 5 TECU in just 3 minutes. The deepest signal fades (refer to Figure 6) were accompanied by repeated cycle slips in the differential carrier phase, which complicates TEC estimation considerably [*Carrano and Groves*, 2006].

One of the more important consequences of the solar radio burst is that the reduction in signal to noise ratio for the GPS satellite signals leads to intermittent loss of lock on the individual satellites. This leads to a reduction in the number of satellites available to compute the receiver position. When fewer than four satellites are available at any given time, a GPS position outage occurs. Moreover, since all of the GPS signals are affected simultaneously by the solar radio burst the chance of a position outage is relatively high, as compared to the case of ionospheric scintillation which usually affects only a few satellite links at a time. Figure 8 shows the number of GPS satellites used by the receiver to compute the position solution during the solar radio burst, measured at a rate of 1 Hz. The longest GPS outage experienced by this receiver was 155 seconds, while the total duration of all the individual outages combined during the solar radio burst was 313 seconds.

Satellites Used in Position Solution
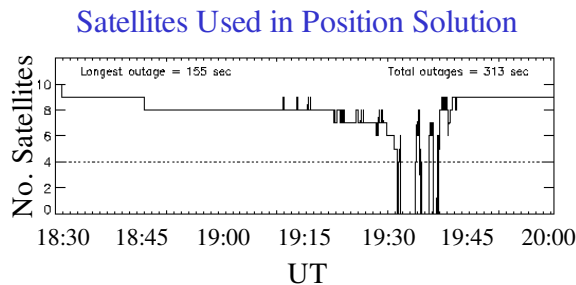
Figure 8. Number of GPS satellites used by the GPS receiver to compute the position solution measured on December 6, 2006 at Ancon with an Ashtech Z-XII GPS receiver, monitored at the rate of 1 Hz.

The horizontal and vertical GPS positioning errors measured during the solar radio burst are shown in Figure 9. The largest horizontal and vertical errors briefly exceeded 20 and 60 meters, respectively, although these errors were typically on the order of 10 meters or less.

GPS Positioning Error
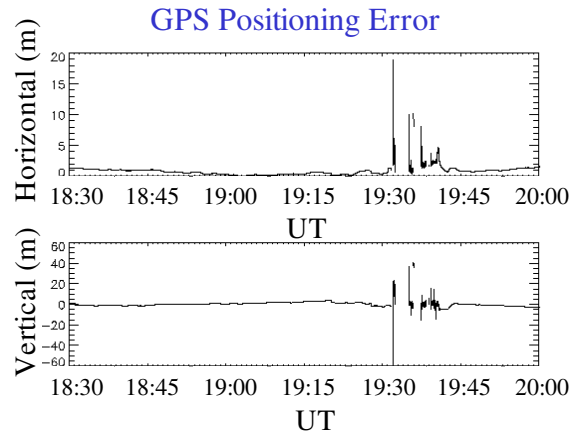
Figure 9. GPS horizontal (top) and vertical (bottom) positioning errors measured on December 6, 2006 at Ancon with an Ashtech Z-XII GPS receiver recording position information at a rate of 1 Hz.

Observations from Kwajalein Atoll

Deep signal fades on L1 and L2 were observed at each of the AFRL-SCINDA GPS receivers located on the sunlit side of the Earth during the December 6, 2006 solar radio burst. In this section, we show measurements from Kwajalein Atoll collected with an Ashtech Z-XII recording data at 20 Hz. The solar incidence (zenith) angle was a much larger 86° from this location, as compared with the GPS receiver at Ancon and, as shown in Figure 10, the corresponding signal fades on L1 and L2 due to the event were smaller at this location. Once again, the pattern of signal fading is nearly identical for each GPS satellite in view, regardless of its elevation or azimuth. The fades are shallower because the solar radio power entered the GPS antenna at a lower grazing angle where the gain of the antenna is less. In the next section we will examine the solar incidence effect in greater detail. The deepest L1 and L2 signal fades observed at Kwajalein were approximately 14 dB and 18 dB, respectively. The longest L1 signal fade was 2 minutes and the longest L2 fade was about 5 minutes. Very few instances of GPS loss of lock were observed at Kwajalein during this solar radio burst due to the large solar incidence angle.

Note that the temporal structure of the GPS signal fades measured at Kwajalein bears a strong similarity to the structure of the signal fades observed at Ancon, particularly after 19:00 UT. The prominent signal fade observed at Ancon near 18:53 UT was not observed at Kwajalein, however, because the solar incidence angle was 94° at this time (this station was rotating into sunlight at this time as dawn approached) and it is very likely that a local obstruction on the ground (such as a building) blocked the radio noise from the sun at this time.

6

L1 ΔC/No

L2 ΔC/No
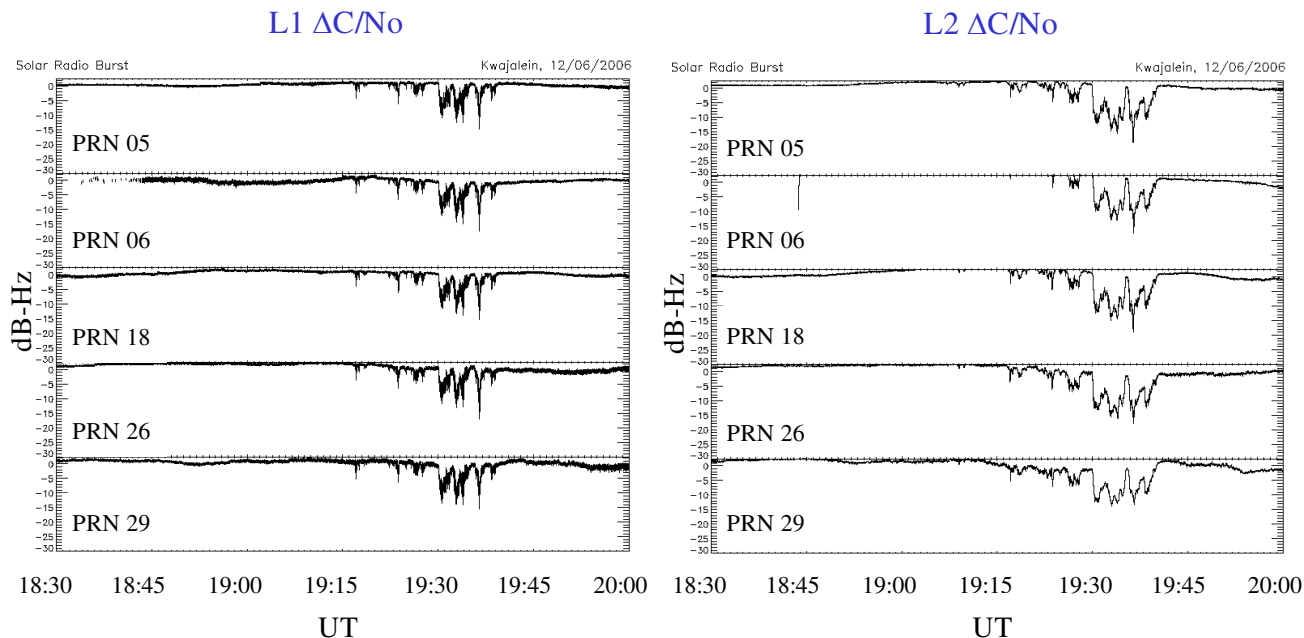
Figure 10. GPS signal fades on the L1 (left) and L2 (right) carriers for a number of GPS satellites observed on December 6, 2006 at Kwajalein Atoll with an Ashtech Z-XII GPS receiver. The solar incidence (zenith) angle at 19:15 UT was approximately 86°.

Differential Pseudorange

Differential Carrier Phase
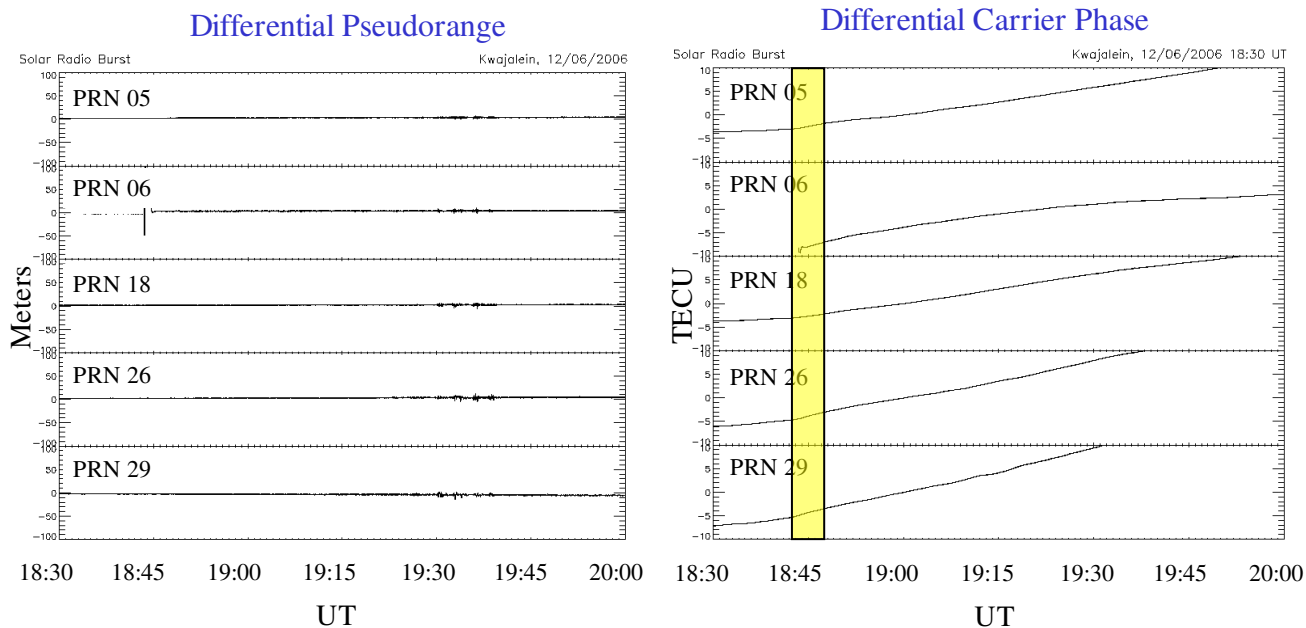
Figure 11. Differential pseudorange (left) and differential carrier phase (right) measured on December 6, 2006 at Kwajalein with an Ashtech Z-XII GPS receiver. The yellow shaded region indicates the SITEC event due to enhanced EUV radiation from the solar flare.

Figure 11 shows the differential pseudorange (in meters) and differential carrier phase (in TEC units) observed at Kwajalein during this event. The fluctuations in the differential pseudorange approached 10 meters during the deepest GPS signal fades, which is smaller than those observed at Ancon but still represent unphysical errors in the receiver's estimation of the pseudorange. The differential carrier phase once again shows an SITEC event starting at the same universal time as it was observed from Ancon, but with less prominence at this high angle of solar incidence. The GPS signal fades at Kwajalein were not accompanied by an excessive rate of cycle slips because of the high solar incidence.

Since there were few loss of lock events observed at Kwajalein as a result of this solar radio burst, the number of satellites used in the position solution was essentially that dictated by the geometry of the GPS constellation at the time and the configuration of ground-based obstructions at the site. Figures 12 and 13 show the number of satellites used in the position solution and the GPS positioning errors observed at Kwajalein during this event, respectively. These results suggest that the solar radio burst had only a moderate, if any, impact on GPS tracking and positioning because of the high solar incidence angle at this station. As we shall show in the next section, greater impacts were observed at stations where the solar incidence angle is smaller.

Satellites Used in Position Solution
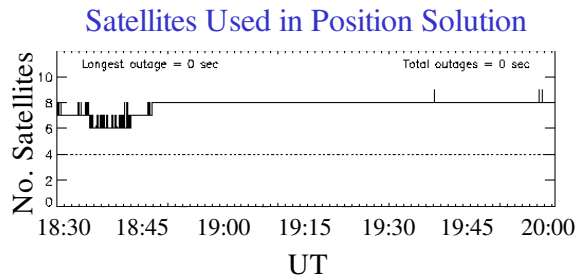
Figure 12. Number of GPS satellites used to compute the position solution on December 6, 2006 at Kwajalein with an Ashtech Z-XII GPS receiver, monitored at a rate of 1 Hz.

GPS Positioning Error
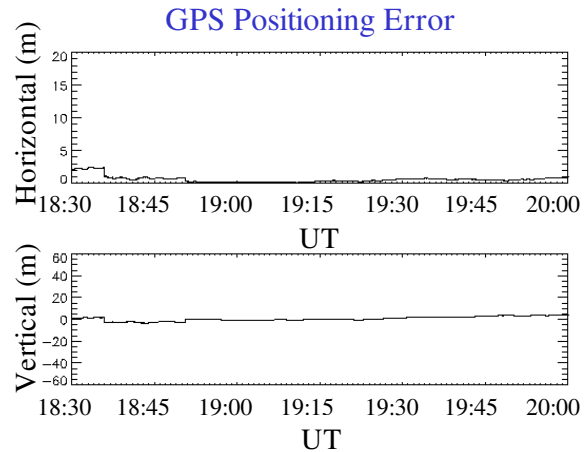
Figure 13. GPS horizontal (top) and vertical (bottom) positioning errors measured on December 6, 2006 at Kwajalein with an Ashtech Z-XII GPS receiver recording position information at a rate of 1 Hz.

Dependence on the Solar Incidence Angle

Both the GPS satellite signals and the solar radio noise processed by the receiver are modulated by the gain of the specific GPS antenna used. The GPS satellite signal is amplified according to the antenna gain at the elevation of the satellite, whereas the solar radio noise is amplified according to the antenna gain at the angle of solar incidence. Therefore, the depth of signal fading due to the solar radio burst should depend on the solar incidence angle. We can use this dependence to estimate the depth of fading that would occur at any arbitrary solar incidence angle.

For example, a simple model for the gain of the Ashtech choke ring antenna which we used to collect the data at Ancon and Kwajalein presented in this paper is graphically illustrated in Figure 14. For this antenna, there is a 9 dB difference between the gain at zenith and the gain at 85° zenith angle and therefore, assuming the AGC loop keeps the input power constant, one may expect the GPS signal fades due to a solar radio burst to be 9 dB deeper at a site located at the subsolar point (where the solar incidence angle is zero) as compared to at a site where the solar incidence angle is 85°.
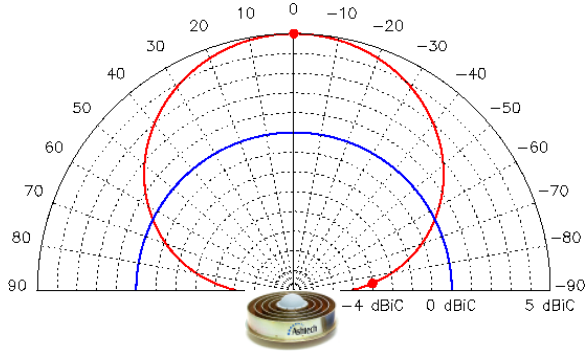
Figure 14. Model gain pattern for the Ashtech choke ring antenna as a function of zenith angle. This antenna has 5 dBiC of gain in the vertical and -4 dBiC of gain at 85° zenith angle. A Gaussian functional form has been used to interpolate the antenna gain between these two points.

We wish to develop an expression for the solar radio burst power and vertical equivalent signal to noise ratio given the GPS signal fades and the local solar incidence angle. We neglect atmospheric attenuation (which is less than 1 dB at L band). Let S represent the power of the broadcast GPS signal for a given satellite, P_N represent the system noise (thermal plus cosmic background) in the absence of solar radio burst power, and g(γ) be the antenna gain as a function of the zenith angle, γ. In the absence of solar radio noise, the signal to noise ratio depends on the satellite elevation as follows:

$$SNR^0(\epsilon)=\frac{S}{P_N}\left[\frac{g(90-\epsilon)}{g(0)}\right] \qquad (1)$$

where ε is the satellite elevation. Now let P_{SRB} represent the RHCP solar radio power at the GPS L1 frequency. We can express the signal to noise ratio of the GPS L1 carrier during the solar radio burst as follows:

$$SNR^0(\epsilon,\theta)=\frac{S\left[\dfrac{g(90-\epsilon)}{g(0)}\right]}{\left[P_N+P_{SRB}\dfrac{g(\theta)}{g(0)}\right]} \qquad (2)$$

where θ is the solar incidence angle. We solve for the solar radio burst power using equations (1) and (2) to obtain

$$P_{SRB}=P_N\frac{g(0)}{g(\theta)}\left[\frac{SNR^0}{SNR}-1\right] \qquad (3)$$

Note that the satellite elevation cancels in this expression, as expected. The ratio SNR/SNR⁰ (which appears in the above in reciprocal form) represents the signal fading due to the solar radio burst, in linear units. Thus, it should be possible to measure the RHCP power of a solar radio burst using a GPS receiver provided the signal fades are large enough to detect and if the system noise can be adequately characterized. In practice, however, P_N is likely to be known only approximately.

At this point, we can determine the vertical equivalent (zenith) signal fading due to the solar radio burst that would be observed if the receiver were located at the sub-solar point (0° solar incidence). To do this we evaluate equation (2) at θ=0 and combine with (3) to arrive for the expression for the vertical equivalent signal fading due to the solar radio burst:

$$SNR^Z(\theta)=\frac{SNR^0}{\left[1+\dfrac{g(0)}{g(\theta)}\left[\dfrac{SNR^0}{SNR}-1\right]\right]} \qquad (4)$$

Note that the system noise cancels in this expression. We can use equation (4) to compare the GPS signal fades from stations where the local solar incidence angles differ. Figure 15 shows the pattern of L1 signal fades due to the solar radio burst on December 6, 2006 as observed from Ancon, Peru; Antofagasta, Chile; Sao Luis, Brazil; and Kwajalein Atoll before and after correcting for the local solar incidence angle. Note how remarkably similar the signal fading patterns are even when measured by GPS receivers separated by thousands of miles. This similarity is even more evident when the vertical equivalent signal fades are compared. As stated earlier, the absence of the large fade at 18:53 UT from the measurement at Kwajalein can be explained by the fact that the solar incidence angle exceeded 90° at this time so that the solar radio noise was likely blocked by a terrestrial object. Similar results were obtained for the L2 carrier signal, shown in Figure 16. The maximum vertical equivalent L1 and L2 signal fades during this event were approximately 27 dB and 30 dB, respectively.

L1 ΔC/No

Vertical Equivalent L1 ΔC/No
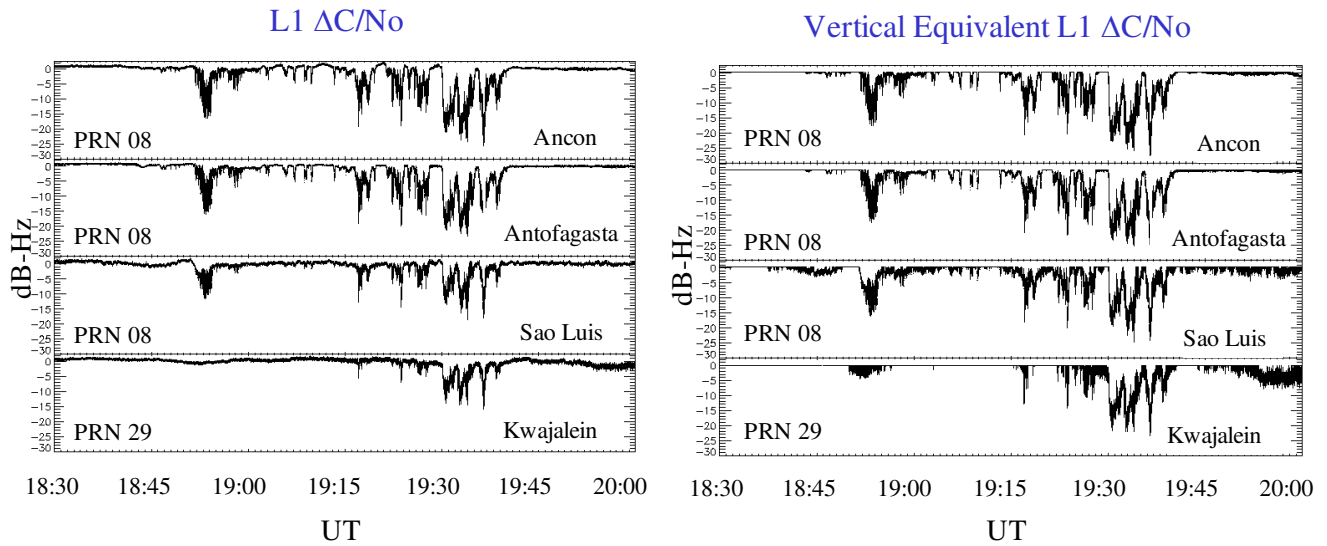
Figure 15. Left panel: GPS L1 signal fades at Ancon, Antofagasta, Sao Luis, and Kwajalein during the December 6, 2006 solar radio burst. The solar incidence angle from these stations are 34°, 37°, 68°, and 86° respectively. Right panel: vertical equivalent GPS L1 signal fades at these same stations.

L2 ΔC/No

Vertical Equivalent L2 ΔC/No
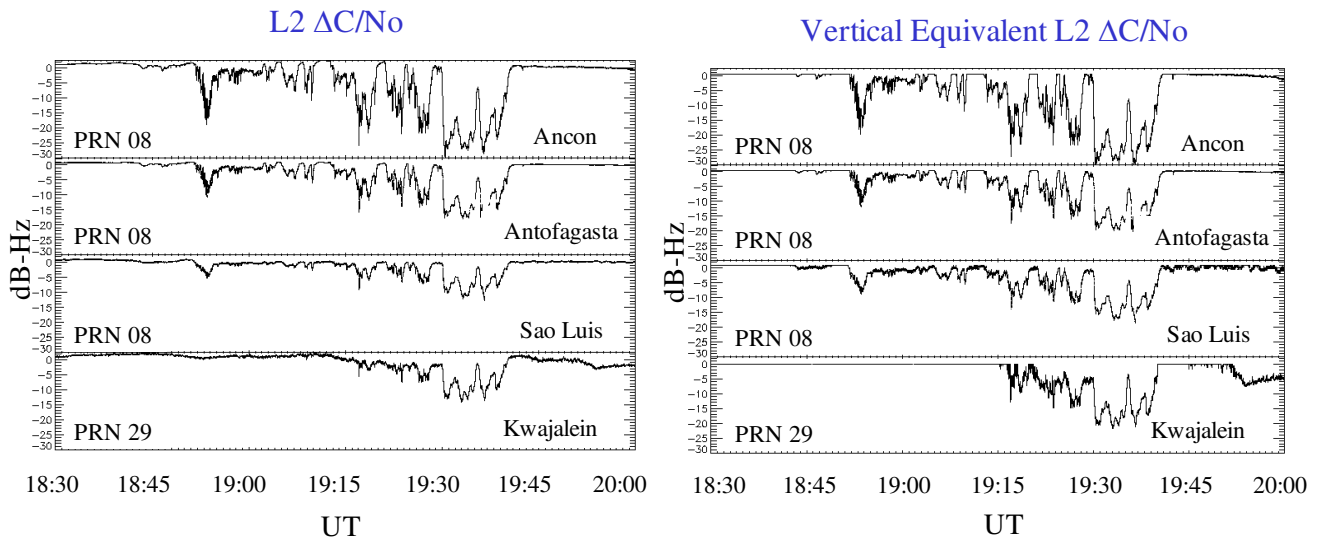
Figure 16. Left panel: GPS L2 signal fades at Ancon, Antofagasta, Sao Luis, and Kwajalein during the December 6, 2006 solar radio burst. The solar incidence angle from these stations are 34°, 37°, 68°, and 86° respectively. Right panel: vertical equivalent GPS L2 signal fades at these same stations.
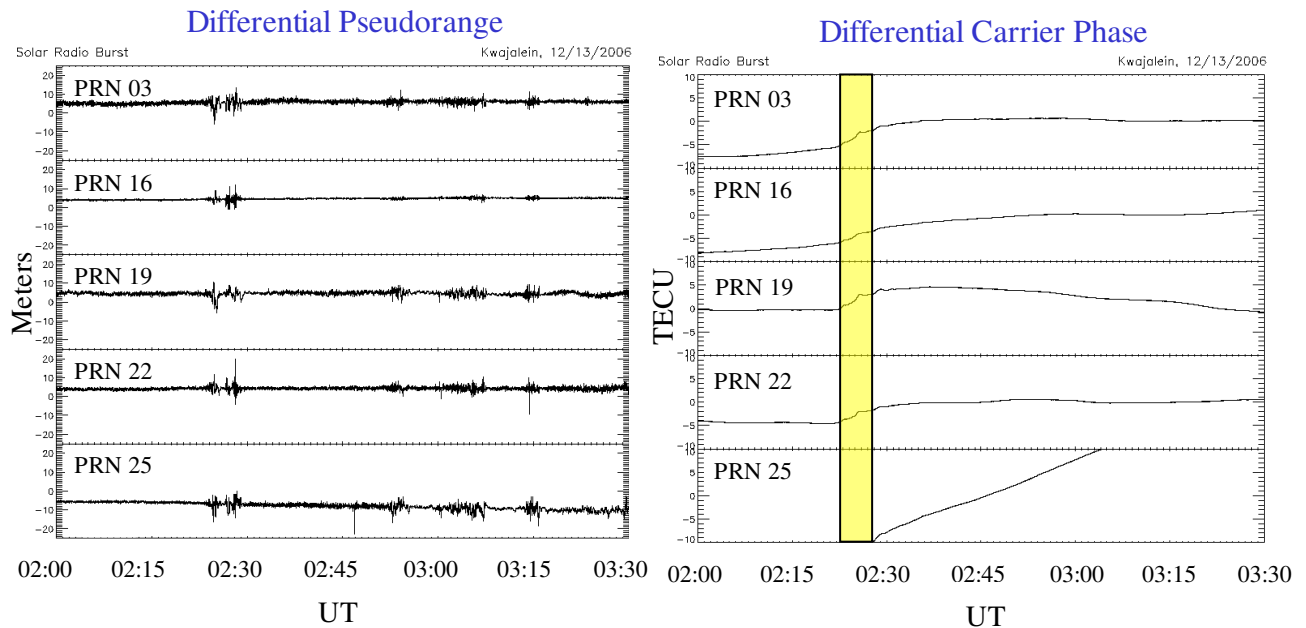
<u>December 13, 2006</u>

The X3.4 solar flare that occurred on December 13, 2006 was also associated with a solar radio burst that caused deep signal fades of the L1 and L2 GPS signals. Figure 17 shows the GPS signal fades on L1 and L2 during this solar radio burst. The solar incidence angle during the event (at the midpoint of the time interval shown) was 44°. The structure of these signal fades resembles that observed on December 6, namely a strong impulse of power near the peak of the X-ray emission, followed by a brief quiet period and then several rapid fades lasting approximately an hour in total. The signal fading patterns are nearly identical for all the GPS satellites regardless of their elevation and azimuth because the solar radio noise enters at the antenna. The deepest fades on L1 and L2 were approximately 19 dB and 25 dB, respectively. The longest fades on L1 and L2 were roughly 5 minutes and 7 minutes, respectively. Few loss of lock events were caused by these signal fades, however.

Figure 18 shows the differential pseudorange (in meters) and differential carrier phase (in TEC units) observed at Kwajalein during the December 13 solar radio burst. The fluctuations in the differential pseudorange were on the order of 5-10 meters during the deepest GPS signal fades and represent unphysical errors in the receiver's estimation of the pseudorange. The differential carrier phase clearly indicates a SITEC event due to the impulsive ionization caused by the solar flare. The SITEC event began at approximately 02:40 UT, and subsequently the TEC increased by about 4 TEC units in 7 minutes. The GPS signal fades were not accompanied by excessive cycle slips.
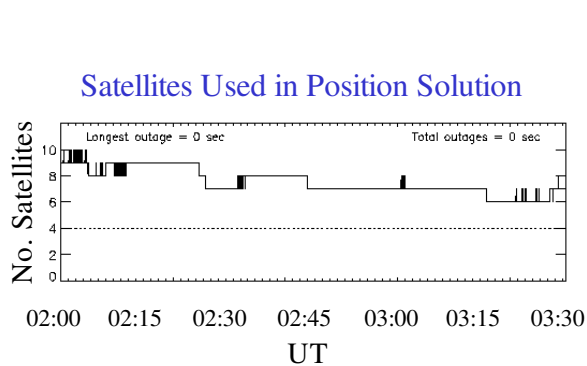
Since few loss of lock events were observed as a result of this solar radio burst, the number of satellites used in the position solution was dictated by the geometry of the constellation at the time and the configuration of ground-based obstructions at the site. Figures 19 and 20 show the number of satellites used in the position solution and the GPS positioning errors observed at Kwajalein during this event, respectively. Despite the relatively deep signal fades observed (refer to Figure 15) during the event, the impact on GPS tracking and positioning accuracy was minimal. No GPS position outages were observed.
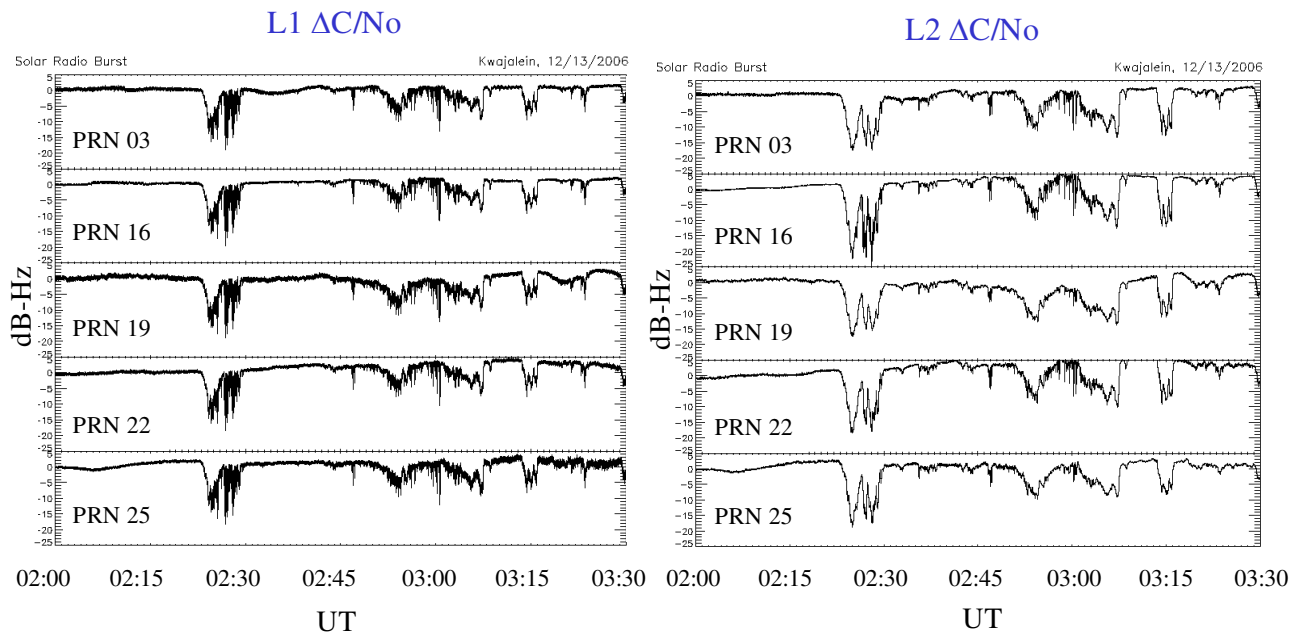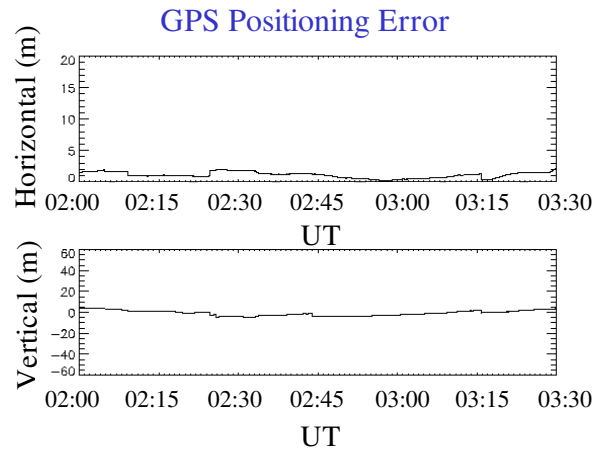

Figure 17. GPS signal fades on L1 (left) and L2 (right) for a number of GPS satellites observed on December 13, 2006 at Kwajalein with an Ashtech Z-XII GPS receiver. The solar incidence (zenith) angle at 02:45 UT was approximately 44°.

11

Differential Pseudorange

Solar Radio Burst   Kwajalein, 12/13/2006

PRN 03

PRN 16

Meters

PRN 19

PRN 22

PRN 25

02:00   02:15   02:30   02:45   03:00   03:15   03:30

UT

Differential Carrier Phase

Solar Radio Burst   Kwajalein, 12/13/2006

PRN 03

PRN 16

TECU

PRN 19

PRN 22

PRN 25

02:00   02:15   02:30   02:45   03:00   03:15   03:30

UT

Figure 18. Differential pseudorange (left) and differential carrier phase (right) measured on December 13, 2006 at Kwajalein with an Ashtech Z-XII GPS receiver. The yellow shaded region indicates the SITEC event due to enhanced EUV radiation from the solar flare.

Satellites Used in Position Solution

No. Satellites

Longest outage = 0 sec   Total outages = 0 sec

02:00   02:15   02:30   02:45   03:00   03:15   03:30

UT

Figure 19. Number of GPS satellites used to compute the position solution on December 13, 2006 at Kwajalein with an Ashtech Z-XII GPS receiver, monitored at a rate of 1 Hz.

GPS Positioning Error

Horizontal (m)

02:00   02:15   02:30   02:45   03:00   03:15   03:30

UT

Vertical (m)

02:00   02:15   02:30   02:45   03:00   03:15   03:30

UT

Figure 20. GPS horizontal (top) and vertical (bottom) positioning errors measured on December 13, 2006 at Kwajalein with an Ashtech Z-XII GPS receiver recording position information at a rate of 1 Hz.

L1 ΔC/No

L2 ΔC/No
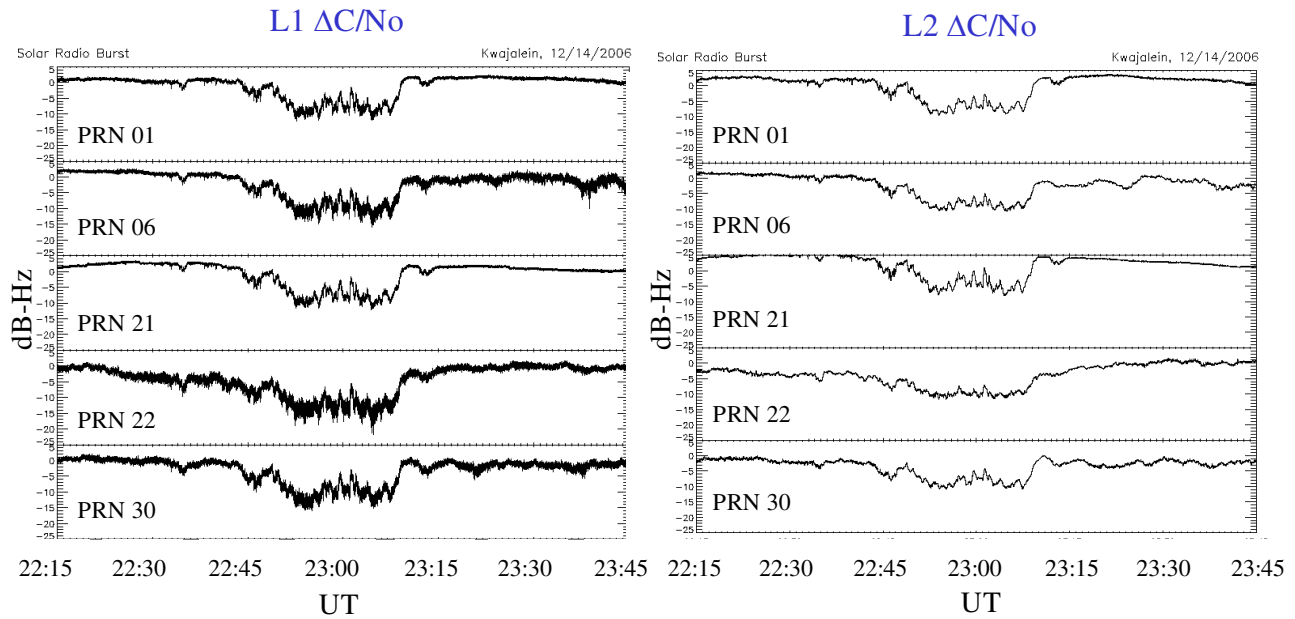
Figure 21. GPS signal fades on L1 (left) and L2 (right) for a number of GPS satellites observed on December 14, 2006 at Kwajalein with an Ashtech Z-XII GPS receiver. The solar incidence (zenith) angle at 23:00 UT was approximately 42°.

December 14, 2006

The X1.5 solar flare that occurred on December 14, 2005 was also associated with a solar radio burst that caused deep signal fades on the L1 and L2 GPS signals. Figure 21 shows the GPS signal fades on L1 and L2 during this solar radio burst. The solar incidence angle was approximately 42° during the event. The structure of the signal fades is somewhat different from that measured on December 6 and 13 in that during this event essentially one fade of extended duration (approximately 25 minutes) was observed. Another notable difference is that the GPS signal fades on L1 are actually deeper than they are on L2. As pointed out by Cerruti [2007], this must have occurred because the level of RHCP solar radio power at the L1 frequency was larger than it was at L2 at this time. Figure 22 shows the RHCP solar radio power measured by the OVSA telescope, which confirms this hypothesis. The fading patterns are nearly identical for all the GPS satellites regardless of their elevation and azimuth. The deepest fades on L1 and L2 were approximately 15 dB and 10 dB, respectively. The longest fades on L1 and L2 were roughly 25 minutes each.
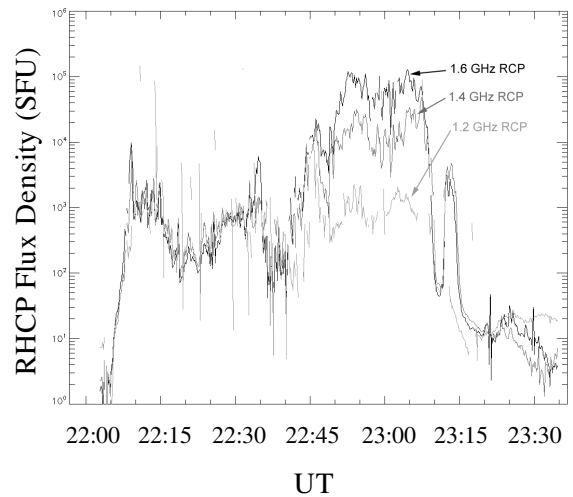

Figure 22. RHCP solar radio power measured at 1.2 GHz, 1.4 GHz, and 1.6 GHz by the OVSA telescope operated by NJIT. Figure courtesy of D. Gary and P. Kintner.

Differential Pseudorange


Differential Carrier Phase
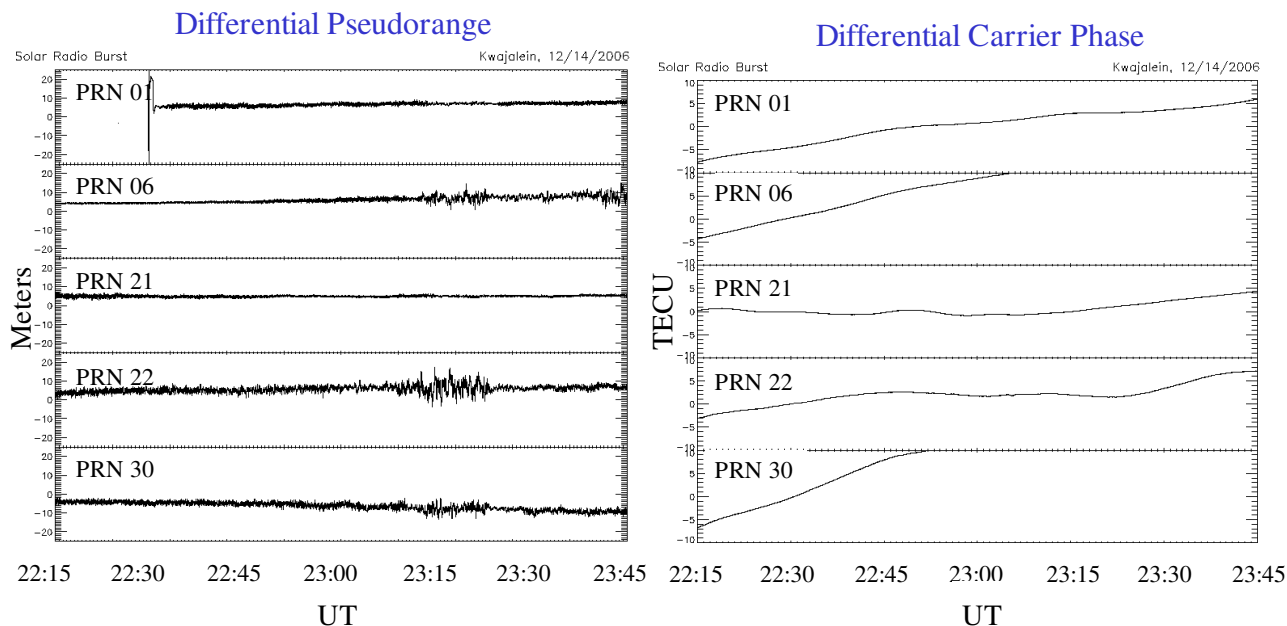
Figure 23. Differential pseudorange (left) and differential carrier phase (right) measured on December 14, 2006 at Kwajalein with an Ashtech Z-XII GPS receiver.

Figure 23 shows the differential pseudorange (in meters) and differential carrier phase (in TEC units) observed at Kwajalein during the December 14, 2006 solar radio burst. Fluctuations in the differential pseudorange approached 15 meters during the event, indicating unphysical errors in the receiver's estimation of the pseudorange. The differential carrier phase showed little evidence of a SITEC event due to the solar flare. The GPS signal fades were not accompanied by excessive cycle slips.

Since there were few loss of lock events observed as a result of this solar radio burst, the number of satellites used in the position solution was dictated by the geometry of the GPS constellation and configuration of ground obstructions at the site. Figures 24 and 25 show the number of satellites used in the position solution and the GPS positioning errors observed at Kwajalein during this event, respectively. Despite the relatively deep signal fades observed (shown in Figure 21) during the event, the impact on GPS tracking and positioning accuracy was minor. No GPS position outages were observed during the event.

Satellites Used in Position Solution
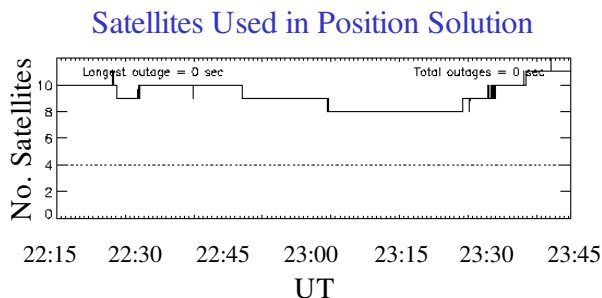
Figure 24. Number of GPS satellites used to compute the position solution on December 14, 2006 at Kwajalein with an Ashtech Z-XII GPS receiver, monitored at a rate of 1 Hz.

14

GPS Positioning Error
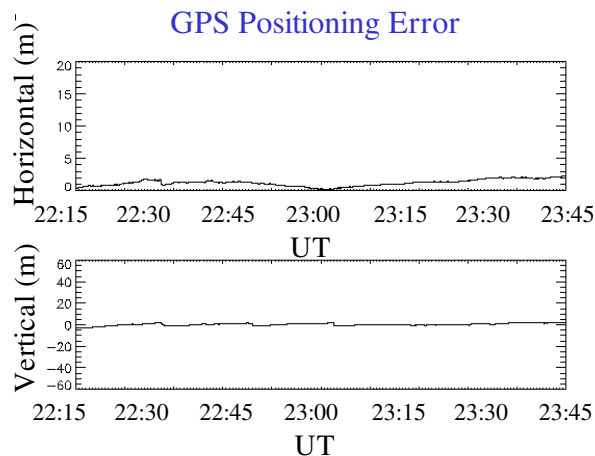
Figure 25. GPS horizontal (top) and vertical (bottom) positioning errors measured on December 14, 2006 at Kwajalein with an Ashtech Z-XII GPS receiver recording position information at a rate of 1 Hz.

5. CONCLUSIONS

We have investigated the effects of the X class solar flares that occurred on December 5, 6, 13, and 14 of 2006 and the associated solar radio bursts on the GPS receivers of the AFRL SCINDA global network. The solar radio burst associated with the X9.0 solar flare on December 5 did not cause a detectable reduction in the signal to noise ratio of the GPS carrier signals. The solar radio bursts on December 6, 13, and 14, on the other hand, radiated enough microwave power and with the proper polarization to cause severe fading of the GPS carrier signals for up to an hour. During these events, nearly identical patterns of intermittent signal fading were observed along all GPS satellite links from all receivers located on the sunlit side of Earth (even from receivers separated by thousands of miles). The depth of the GPS signal fades were modulated by the local solar incidence angle due to the zenith angle dependence of the GPS antenna gain. It should be emphasized, however, that the signal fades observed were caused by the response of the Automatic Gain Control (AGC) circuitry of the receiver, which acts to reduce the total signal received at the antenna. The total signal received at the antenna had actually increased due to the addition of noise from the solar radio bursts.

We have derived an expression for the vertical equivalent GPS signal fading due to a solar radio burst (i.e. the signal fading that would occur if the receiver were located at the subsolar point) in order to compare measurements collected at locations with different solar incidence angles. We estimate the

maximum vertical equivalent GPS signal fading at L1 during the December 6 event to be 27 dB.

Although the December 13 and 14 solar radio bursts resulted in deep fading of the GPS signals, their impacts on GPS tracking and positioning accuracy were minimal. The December 6 solar radio burst, on the contrary, was particularly intense and caused profound impacts on GPS performance. During this event, GPS receivers experienced difficulty tracking and incurred large ranging errors associated with the signal fading and intermittent loss of code lock. These combined factors led to elevated GPS positioning errors of up to 20 and 60 meters in the horizontal and vertical directions, respectively. The total duration of GPS position outage periods, during which no position solution is available, exceeded 5 minutes during this event.

SITEC events were observed in conjunction with the solar flares, at rates approaching 0.5-1.0 TEC/min. These rates were likely also related to the solar incidence angle, although the effect of changing slant paths through the ionosphere due to differing satellite elevations were not taken into account.

It is worth noting that these powerful solar radio bursts occurred, somewhat surprisingly, during solar minimum. If solar radio bursts with significant power in the gigahertz frequency range are more prevalent during solar maximum conditions when the sun is more active this could suggest that solar radio burst impacts on GPS operations may be more severe and occur more frequently than previously anticipated.

6. ACKNOWLEDGMENTS

7. REFERENCES

Carrano, C., K. Groves, and J. Griffin, 2005, Empirical Characterization and Modeling of GPS Positioning Errors Due to Ionospheric Scintillation, Ionospheric Effects Symposium, Alexandria, VA, May 3-5.

Carrano, C., and K. Groves, 2006, The GPS segment of the AFRL-SCINDA global network and the

challenges of real-time TEC estimation in the equatorial ionosphere, Proceedings of the Institute of Navigation, National Technical Meeting, Monterey, CA.

Carrano, C., 2008, GPS-SCINDA: a real-time GPS data acquisition and ionospheric analysis system for SCINDA, to be submitted for publication as an AFRL technical report.

Cerruti A. P., P. M. Kintner, D. E. Gary, L. J. Lanzerotti, E. R. de Paula, H. B. Vo, 2006, Observed solar radio burst effects on GPS/Wide Area Augmentation System carrier-to-noise ratio, *Space Weather*, 4, S10006, doi:10.1029/2006SW000254.

Cerruti, A., 2007, Space Weather and GPS website, http://gps.ece.cornell.edu/spaceweather.html.

Kintner, A., 2007, GPS Receiver Operation and the Solar Radio Burst of December 6, 2006, comments made during presentation at the Beacon Satellite Symposium, June 11-17, Boston, MA.

Groves, K., S. Basu, E. Weber, M. Smitham, H. Kuenzler, C. Valladares, R. Sheehan, E. MacKenzie, J. Secan, P. Ning, W. McNeil, D. Moonan, and M. Kendra, 1997, Equatorial scintillation and systems support, *Radio Sci.*, 32, 2047.

Klobuchar, J. A., J. M. Kunches, and A. J. Van Dierendonck, 1999, Eye on the ionosphere: potential solar radio burst effects on GPS signal to noise, *GPS Solutions*, 3, 69-71.

Warmuth, A. and G. Mann, 2005, The application of radio diagnostics to the study of the solar drivers of space weather, *Lect. Notes Phys.* 656, 51-70.